Supporting Information

Experimental Section

All chemicals were used as received without purification. $Zn(NO_3)_2 \cdot 6H_2O$ (99%), $Co(NO_3)_2 \cdot 6H_2O$ (99%) and 2-Methylimidazole were purchased from Aladdin. 1,3-Dioxlane(DOL) (99.5%),1,2-Dimethoxyethane(DME) (99.5%), $LiNO_3$(99.9%), Li_2S and sublimed sulfur power were purchased from Alfa Aesar. Graphene oxide suspension was synthesized by Hummer's method using natural flake graphite.

Preparation of Zn/Co-ZIF nanosheets

For the preparation of Zn/Co-ZIF-B nanosheets, 1.116 g $Zn(NO_3)_2 \cdot 6H_2O$ (99%), 1.092 g $Co(NO_3)_2 \cdot 6H_2O$ and 1.232 g 2-methylimidazole were first into three different beakers with 20 ml, 20 ml and 15 ml methanol respectively. The $Co(NO_3)_2 \cdot 6H_2O$/methanol mixed solution was then added to the 2-methylimidazole/methanol solution drop by drop. After ultrasonic, the $Zn(NO_3)_2 \cdot 6H_2O$/methanol mixed solution was then added to the mixed solution, and ultrasonic for 15 min and standing for 30 min. Then, the suspension was transferred to a Teflon-lined stainless steel autoclave and stayed at 120 ℃ for 24 h. After the reaction was finished, the sample washed by centrifugation with methanol for 3 times. The obtained samples were redispered with methanol and ultrasonic for 30 min. The final sample Zn/Co-ZIF nanosheets were obtained after dry for 1 day at 60 ℃. The Zn/Co-ZIF nanosheets with different Zn and Co ratio were prepared by adjusting the ratio of $Zn(NO_3)_2 \cdot 6H_2O$ and $Co(NO_3)_2 \cdot 6H_2O$.

Preparation of the Zn/Co-ZIF@PP separator

50 mg of Zn/Co-ZIF nanosheets was dispersed into 50 mL of ethanol by ultrasonication for subsequent use. Then, 2.5 ml of the Zn/Co-ZIF nanosheets dispersion were re-dispersed to 100 ml of ethanol by ultrasonication for 30 min. The as-prepared dispersion was vacuum filtered on the PP separator (The Vacuum suction filtration area is 17 cm^{-2}). The obtained Zn/Co-ZIF@PP separator was dried at 60 °C for 8 h. The separators modified by ZIF nanosheets with different Zn/Co ratios were prepared by the same method and the areal loading of the modified layer was controlled to be 0.1 mg cm^{-2}.

Preparation of the S/rGO cathode

1.5 mg of graphene oxide, 0.069 ml sodium thiosulfate (1 mol L^{-1}) and 0.069 ml hydrochloric acid (2 mol L^{-1}) were mixed in deionized water to obtain 1.4 ml solution in a vial. After reacted for 2 h at RT, 0.1 ml sodium ascorbate was added to the solution and transfer to the oven with a temperature of 95 °C for 2 h, the obtained hydrogel was washed for 3 times by deionized water and then freeze-dried to get the freestanding S/rGO composite. The areal sulfur loadings are 2.5 mg cm^{-2} for the routine electrochemical performance test. The areal loading of S/rGO depends on the molar mass of sodium thiosulfate and hydrochloric acid. As for the S/rGO with a high sulfur loading of 5.3 mg cm^{-2}, the sodium thiosulfate and hydrochloric acid are changed to

0.140 ml.

Materials Characterization

X-ray diffraction (XRD) characterization was performed to investigate the crystallographic information of samples using a D8 Advance X-ray diffractometer with a non-monochromated Cu Ka X-ray source (λ= 1.054056 Å). Scanning electron microscopic (SEM) images were collected by using a JEOL JSM-7100F at an acceleration voltage of 15 kV. Transmission electron microscopic (TEM) and high-resolution TEM (HRTEM) images were recorded with a Titan G2 60-300 with EDS image corrector. The AFM was performed into this sample using a Nanoscope V Multimode 8 scanning probe microscope from Bruker Corporation. All experiments were carried out with the same AFM probe under ambient conditions (temperature of 25℃, relative humidity of 25%). The Inductively Coupled Plasma Optical Emission Spectr (ICP) measurement was recorded with a PerkinElmer Optima 4300DV spectrometer.

Separator Characterization

The Dynamic contact angle measurements were conducted using an optical contact angle measuring and contour analysis system (Dataphysics DCA 35). The tensile property was tested using a Instron, USA Electronic universal material Tester (5967) with the constant speed of 50 μm min^{-1} using a load cell of 1 kN. The ~27 μm-thick membrane was cut to a ribbon with width of 1 cm and length of ~8 cm. The Heat resistance was tested by using an Infrared thermal imager (FLIR T429) with a temperature range from 30 °C to 150 °C.

Electrochemical Measurement

CR2025 type coin cells were assembled in an argon filled glovebox. And the contents of water and oxygen were both below 0.1 ppm. The mechanically pressed S/rGO samples with thickness around 100 μm were directly used as the cathode, and lithium foil was used as anode. The electrolyte was a solution of 1M LiTFSI in (1:1) DEM and DOL, and $LiNO_3$(1wt %) was severed as an additive. The ratio of electrolyte to S is 20 (μL):1 (mg). The Galvanostatic charge/discharge cycling was carried out in a CT 2001A multichannel battery testing system (Wuhan LAND Electronic Co, Ltd) with a potential range of 1.7–2.8 V vs. Li/Li^+. The cycle cyclic voltammetry (CV) curves and electrochemical impedance spectroscopy tests (0.1 Hz-100 kHz, 5 mV) were conducted on an electrochemical workstation (Autolab PGSTAT302N). The GITT was carried out under the current pulse and maintained for 30 min to obtain the open-circuit voltages (OCV) and then subsequently rested for 1 h to acquire the quasi-open-circuit-voltage (QOCV) at 0.05 C.

Measurement for the nucleation of lithium sulfide

A Li_2S_8 solution was used as the electrolyte and was prepared by combining stoichiometric amounts of lithium sulfide and sulfur powder in tetraglyme under vigorous magnetic stirring. The freestanding 3D rGO was used as a cathode host to load

the different ZIF nanosheets (areal loading ~1.0 mg cm^{-2}) and a lithium foil was used as the anode to assemble the cell. During the cell assembly process, Li_2S_8 was dropped onto the cathode and then electrolyte without Li_2S_8 was dropped on the lithium anode side. The cell was galvanostatically discharged to 2.06 V under a current of 0.112 mA, and the potential was then kept at 2.05 V until the current dropped below 10^{-5} A. Driven by an overpotential of 0.01 V, Li_2S was deposited and it grew on the rGO surface. Based on Faraday's law, the energy was gathered to evaluate the nucleation/growth rate of lithium sulfide on the rGO/ZIF composite.

Theoretical Calculation Method

The present first principle DFT calculations are performed by Vienna Ab initio Simulation Package(VASP) [1] with the projector augmented wave (PAW) method [2]. The exchange-functional is treated using the generalized gradient approximation (GGA) of Perdew-Burke-Ernzerhof (PBE) [3] functional. The energy cutoff for the plane wave basis expansion was set to 450 eV and the force on each atom less than 0.02 eV/Å was set for convergence criterion of geometry relaxation. The Brillouin zone integration is performed using 1×1×1 k-point sampling. The self-consistent calculations apply a convergence energy threshold of 10^{-4} eV. The DFT-D3 method was employed to consider the van der Waals interaction [4].

The adsorption energy of Li_2S_X molecules was calculated according to

$$E(ads)=E(total)-E(sub)-E(Li_2S_X \text{ or } S_8)$$

where E(ads) is the bonding energy to the Li_2S_X. E(total) is the total energy of the Li_2S_X adsorbed on the substrate, E(sub) and E(Li_2S_X or S_8) are the energies of the substrate and the isolated molecule, respectively.

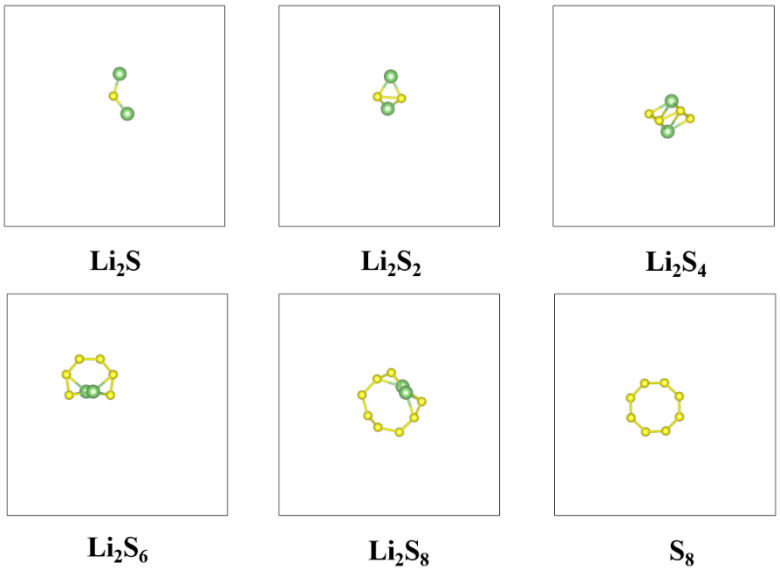

FIGURE S1 DFT molecular skeletons of Li_2S_n and S_8.

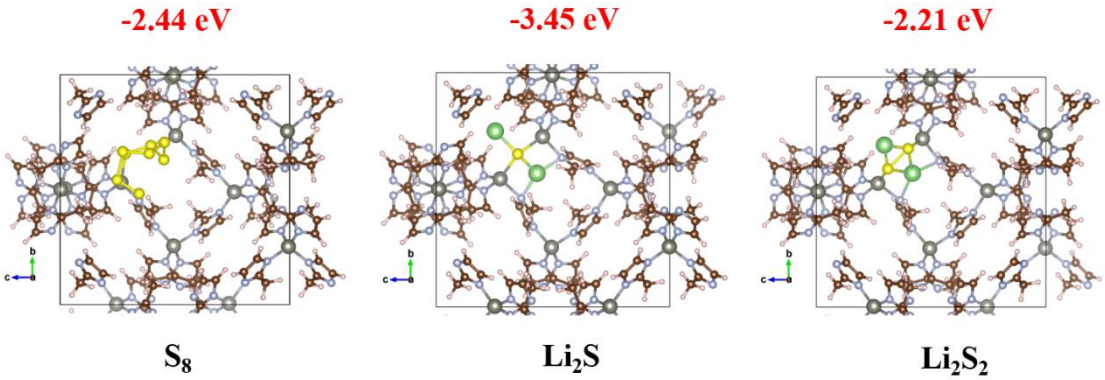

FIGURE S2 Optimized configurations for the binding of short-chain Li_2Sn and S_8 to ZIF-8.

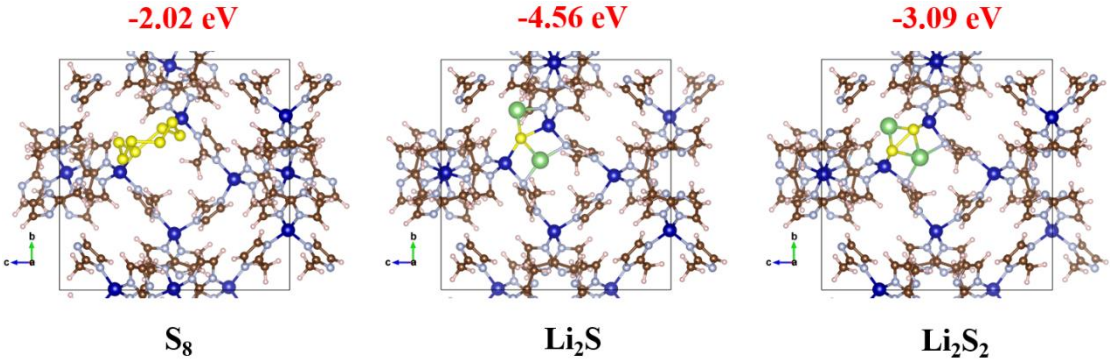

FIGURE S3 Optimized configurations for the binding of short-chain Li_2Sn and S_8 to ZIF-67.

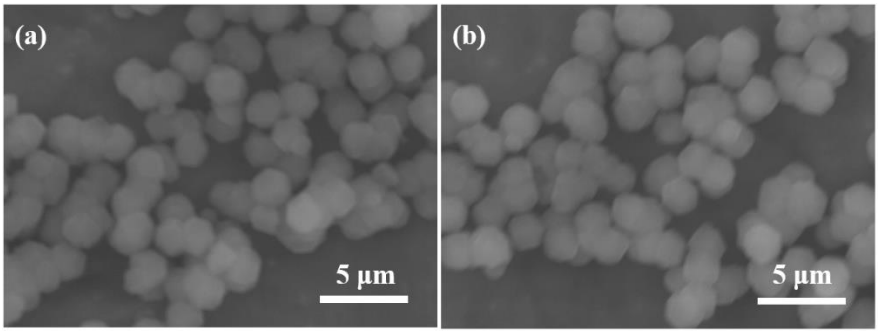

FIGURE S4 The SEM image of Zn/Co-ZIF nanopracticles.

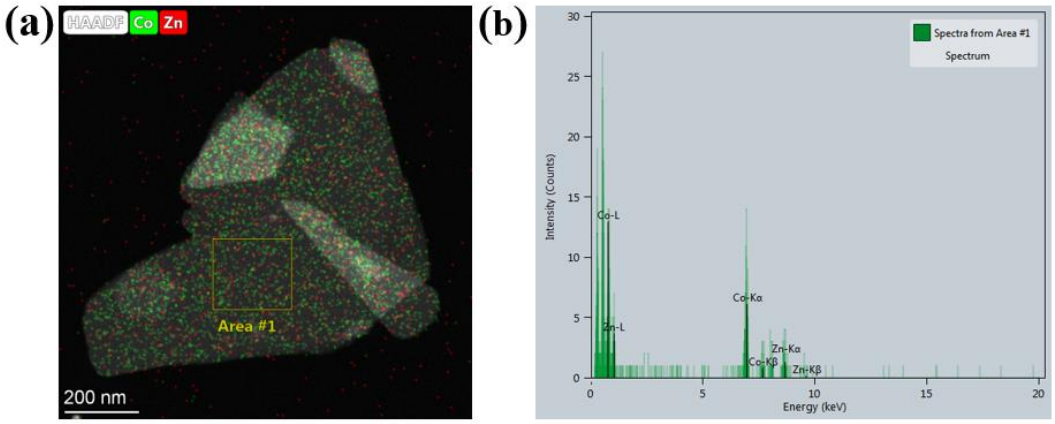

FIGURE S5 (a) The HAADF image of Zn/Co-ZIF nanosheets and (b) the spectrum of corresponding elements.

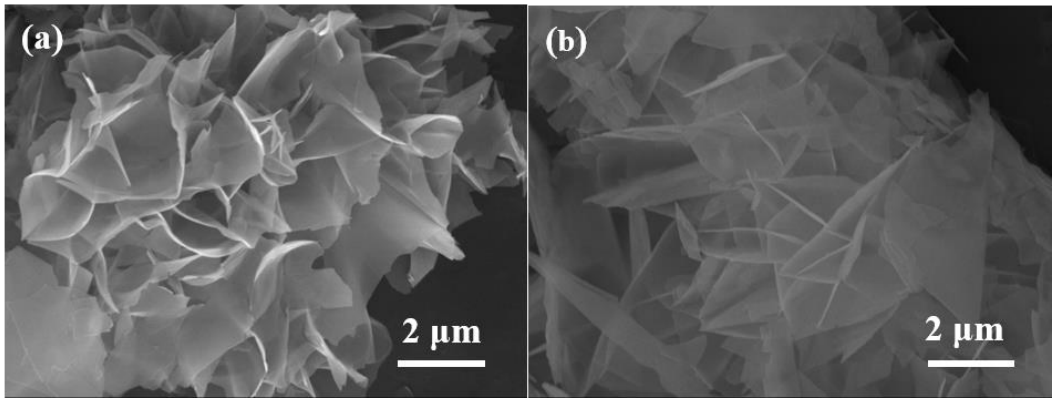

FIGURE S6 The SEM images of (a) ZIF-A and (b) ZIF-C.

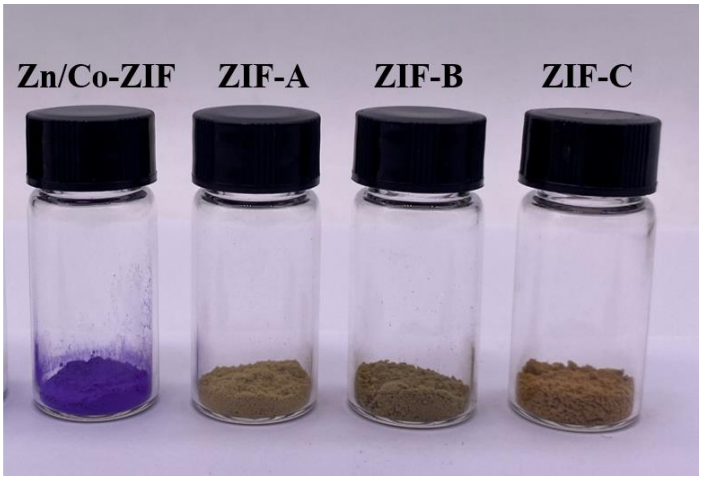

FIGURE S7 The Optical picture of Zn/Co-ZIF nanopracticles, ZIF-A, ZIF-B and ZIF-C nanosheets.

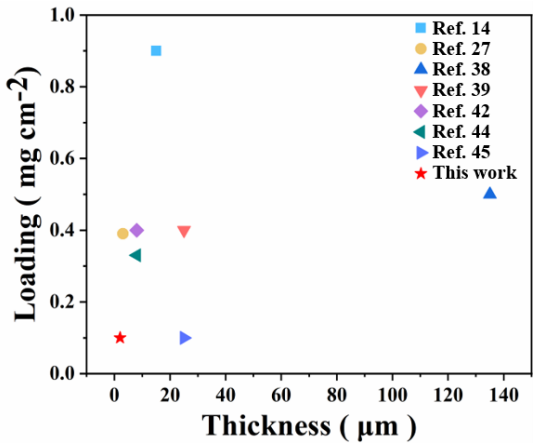

FIGURE S8 The thickness and loadings of different MOF based swparators.

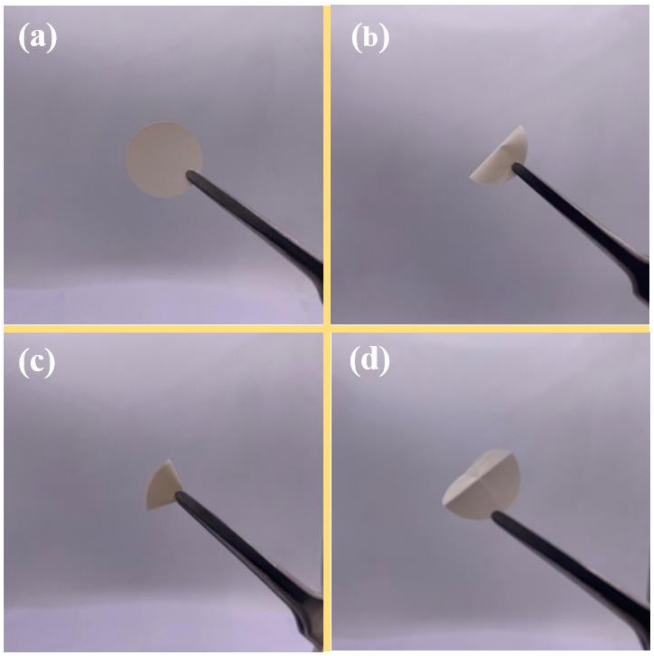

FIGURE S9 (a-d) The Optical picture of Zn/Co-ZIF@PP separator before and after folding.

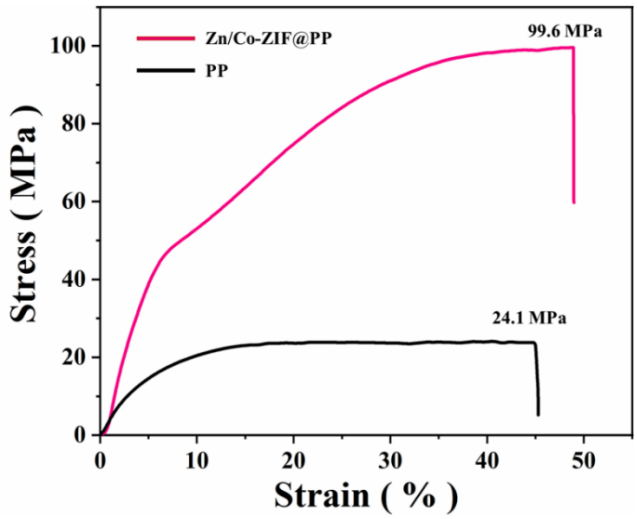

FIGURE S10 Stress-strain curves of PP and Zn/Co-ZIF@PP separators.

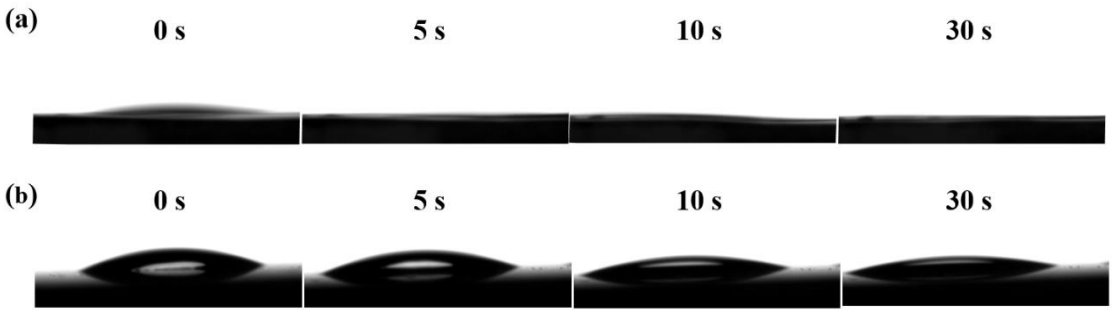

FIGURE S11 Dynamic contact angle measurements with electrolyte for (a) Zn/Co-ZIF@PP separator; (b) PP separator.

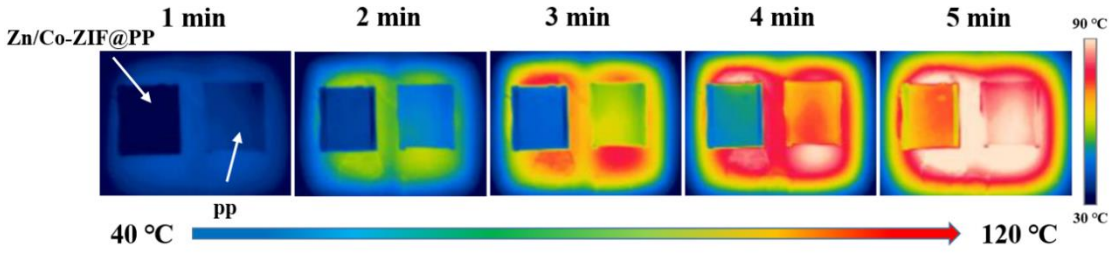

FIGURE S12 Thermal imaging photographs of Zn/Co-ZIF@PP and PP separators heated from room temperature to 120 °C.

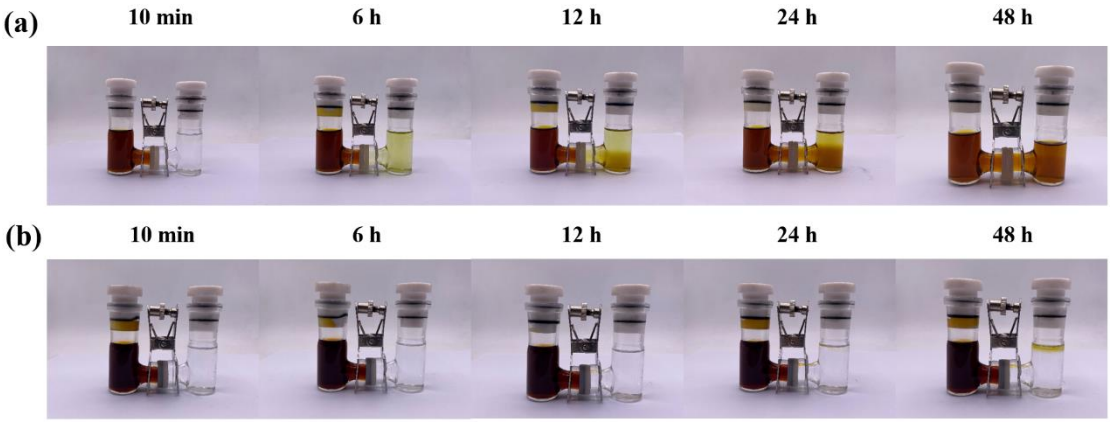

FIGURE S13 Permeation experiments with a double-L device for (a) PP and (b) Zn/Co-ZIF@PP separators.

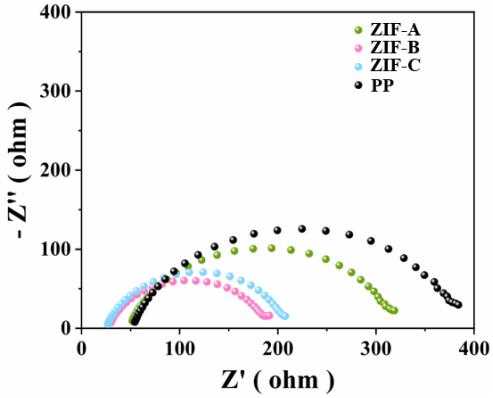

FIGURE S14 The electrochemical impedance spectroscopic (EIS) spectra of Li-S battery assembled with different separators.

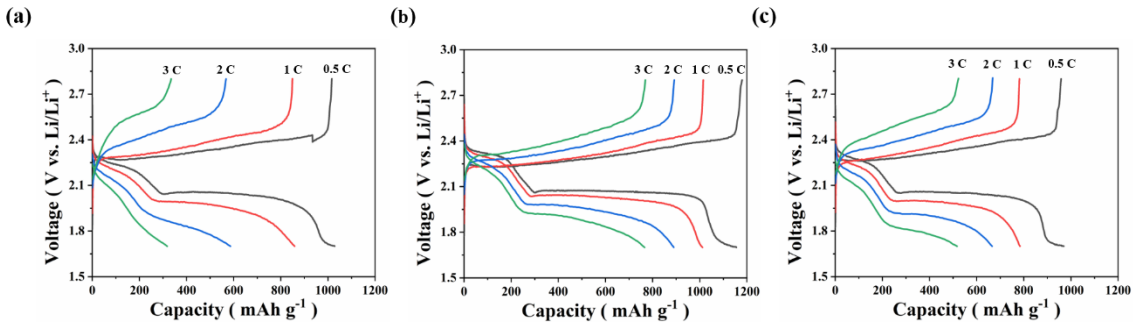

FIGURE S15 The constant current charge/discharge voltage curves of different rate for (a) ZIF-A, (b) ZIF-B, and (c) ZIF-C.

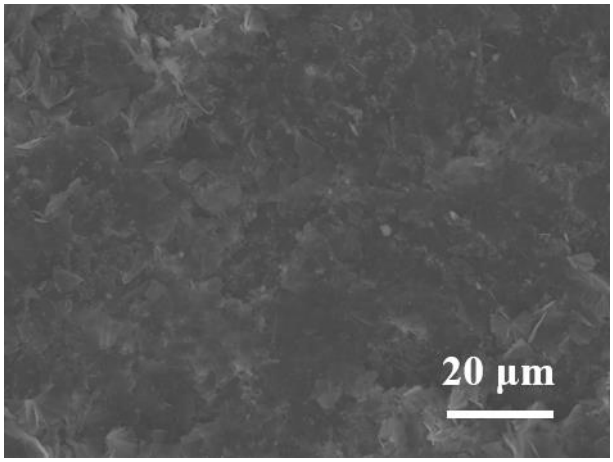

FIGURE S16 The SEM image of the ZIF-B modified separator after cycling.

Table S1 The ICP test results of Zn and Co contents in different ZIF samples

Sample	Zn concentration (µg g^{-1})	Co concentration (µg g^{-1})	Zn:Co (mole ratio)
ZIF-A	909640.3	456775.2	1.8
ZIF-B	356259.1	286236.3	0.9
ZIF-C	441804.6	845380.9	0.5

Table S2 Detailed information of Li-S batteries fabricated with MOF based separators.

MOFs	Thickness (μm)	Coating layer Loadings (mg cm^{-2})	Areal sulfur loading (mg cm^{-2})	Maximum capacity (mAh g-1)	Rate capacity (mAh g^{-1})	Cycle performance		Ref.
						Cycle Number	Fading rate (%)	
HKUST-1	N/A	0.12	2.4	1316 (0.5 C)	963 (2.0 C)	1000 (1.0 C)	0.022	[11]
						1000 (2.0 C)	0.026	
MIL-125(Ti)	20	N/A	2.0	1218 (0.2 C)	592 (2.0 C)	200 (0.2 C)	0.202	[12]
UIO-66	20	N/A	1.5	1120 (0.1 C)	461 (2.0 C)	500 (0.5 C)	0.086	[13]
ZIF-8	15	0.9	1.2	1655 (0.1 C)	583 (2.0 C)	100 (0.2 C)	0.367	[14]
ZIF-67	3	0.39	3.0-3.5	1400 (0.2 C)	400 (3.2 C)	1700 (2 C)	0.015	[27]
ZIF-67	135	0.5	2.6	1302 (0.5 C)	485 (5.0 C)	600 (5.0 C)	0.032	[38]
Co-BTC	25	0.4	1.5	1138 (0.1 C)	478 (5.0 C)	600 (1.0 C)	0.070	[39]
Ce-MOF	8	0.4	2.5	1141 (0.2 C)	663 (4.0 C)	800 (1.0 C)	0.022	[42]
HKUST-1	15	N/A	0.3	1072 (0.2 C)	488 (3.0 C)	500 (0.5 C)	0.058	[43]
$Ni_3(HITP)_2$	8	0.33	N/A	1220 (0.1 C)	800 (2.0 C)	300 (0.5 C)	0.117	[44]
Cu_2(CuTCPP)	25	0.1	2.0	953 (0.2 C)	437 (5.0 C)	900 (1.0 C)	0.032	[45]
UiO-66/SO_3Li	300	N/A	2.0	1069 (0.1 C)	552 (5.0 C)	500 (0.5 C)	0.056	[46]
Zn/Co-ZIF	2	0.1	2.1	1304 (0.5 C)	788 (3.0 C)	1000 (2.0 C)	0.025	This work